Cellular/Molecular

Activation of BK and SK Channels by Efferent Synapses on Outer Hair Cells in High-Frequency Regions of the Rodent Cochlea

Kevin N. Rohmann,[1]* Eric Wersinger,[1]* Jeremy P. Braude,[2] Sonja J. Pyott,[2] and Paul Albert Fuchs[1]

[1]Department of Otolaryngology Head and Neck Surgery, Center for Hearing and Balance, and Center for Sensory Biology, Johns Hopkins University School of Medicine, Baltimore, Maryland 21231 and [2]Department of Biology and Marine Biology, University of North Carolina Wilmington, Wilmington, North Carolina 28403

Cholinergic neurons of the brainstem olivary complex project to and inhibit outer hair cells (OHCs), refining acoustic sensitivity of the mammalian cochlea. In all vertebrate hair cells studied to date, cholinergic inhibition results from the combined action of ionotropic acetylcholine receptors and associated calcium-activated potassium channels. Although inhibition was thought to involve exclusively small conductance (SK potassium channels), recent findings have shown that BK channels also contribute to inhibition in basal, high-frequency OHCs after the onset of hearing. Here we show that the waveform of randomly timed IPSCs (evoked by high extracellular potassium) in high-frequency OHCs is altered by blockade of either SK or BK channels, with BK channels supporting faster synaptic waveforms and SK channels supporting slower synaptic waveforms. Consistent with these findings, IPSCs recorded from high-frequency OHCs that express BK channels are briefer than IPSCs recorded from low-frequency (apical) OHCs that do not express BK channels and from immature high-frequency OHCs before the developmental onset of BK channel expression. Likewise, OHCs of BK$\alpha^{-/-}$ mice lacking the pore-forming α-subunit of BK channels have longer IPSCs than do the OHCs of BK$\alpha^{+/+}$ littermates. Furthermore, serial reconstruction of electron micrographs showed that postsynaptic cisterns of BK$\alpha^{-/-}$ OHCs were smaller than those of BK$\alpha^{+/+}$ OHCs, and immunofluorescent quantification showed that efferent presynaptic terminals of BK$\alpha^{-/-}$ OHCs were smaller than those of BK$\alpha^{+/+}$ OHCs. Together, these findings indicate that BK channels contribute to postsynaptic function, and influence the structural maturation of efferent-OHC synapses.

Key words: **BK channel; cholinergic inhibition; cochlea; efferent inhibition; outer hair cell; SK channel**

Introduction

Calcium-activated potassium channels modulate the excitability of neurons and muscle (Berkefeld et al., 2010). These channels fall into two broad categories, small conductance calcium-activated SK channels (Bond et al., 2005) and large conductance, voltage-gated, calcium-sensitive BK channels (Lee and Cui, 2010). SK and BK channels are distinguished by significant differences in voltage sensitivity, single-channel conductance, calcium affinity, and gating kinetics. Compared with voltage-gated BK channels, voltage-insensitive SK channels have higher calcium affinities and longer mean open times (Bond et al., 2005). Cholinergic inhibition of most sensory hair cells involves activation of SK channels associated with ionotropic ACh receptors containing $\alpha9\alpha10$-subunits (Elgoyhen et al., 1994, 2001) through which calcium enters to activate SK channels and hyperpolarize the hair cells (Housley and Ashmore, 1991; Shigemoto and Ohmori, 1991; Fuchs and Murrow, 1992; Evans, 1996). However, recent work has shown by immunofluorescence that BK channels can be found near efferent synapses on cochlear outer hair cells (OHCs; Engel et al., 2006). *In vitro* examination using intracellular recordings and quantitative immunofluorescence confirmed that BK channels are present only in OHCs from cochlear (high-frequency) middle and basal turns of rats aged P21, where they contribute to ACh-evoked as well as voltage-gated membrane currents (Wersinger et al., 2010). *In vivo* examination corroborates the contribution of BK channels to the efferent suppression of OHCs (Maison et al., 2013).

The initial *in vitro* studies (Wersinger et al., 2010) relied on application of ACh from a puffer pipette that provided long-

Received July 9, 2014; revised Oct. 20, 2014; accepted Dec. 1, 2014.

Author contributions: K.N.R., E.W., S.J.P., and P.A.F. designed research; K.N.R., E.W., J.P.B., and S.J.P. performed research; K.N.R., E.W., J.P.B., S.J.P., and P.A.F. analyzed data; K.N.R., E.W., S.J.P., and P.A.F. wrote the paper.

This work was supported by National Institute on Deafness and Other Communication Disorders (R01 DC001508 to P.A.F.) and P30 DC005211 and T32000023 to the Center for Hearing and Balance at Johns Hopkins University School of Medicine, and a research grant from the Deafness Research Foundation to S.J.P. We thank H. Hiel and M. Lehar for assistance with electron microscopy, G. Zanoto for assistance with confocal microscopy, K. Prestage and I. Campos for assistance with quantification of immunofluorescent data, and Dr. A.L. Meredith (University of Maryland) for providing breeding pairs of BK $^{+/-}$ mice.

*K.N.R. and E.W. contributed equally to this work.

The authors declare no competing financial interests.

E. Wersinger's present address: Sensorion, 650 rue Henri Becquerel, 34000 Montpellier, France.

S. Pyott's present address: Department of Otorhinolaryngology, Head & Neck Surgery University Medical Center Groningen, University of Groningen, P.O. Box 30001, Groningen, RB 9700, The Netherlands.

Correspondence should be addressed to P.A. Fuchs, Department of Otolaryngology Head and Neck Surgery, Center for Hearing and Balance, and Center for Sensory Biology, Johns Hopkins University School of Medicine, Baltimore, MD 21231. E-mail: pfuchs1@jhmi.edu.

DOI:10.1523/JNEUROSCI.2790-14.2015

 0270-6474/15/351821-10$15.00/0

lasting and presumably greater calcium influx than that occurring during synaptic release of ACh. In the present study, the role of BK and SK channels in synaptic function per se was evaluated by examining the contribution of these channels to synaptic currents produced by the stochastic vesicular release of ACh from efferent endings depolarized by elevated extracellular potassium. By combining pharmacological, developmental, and genetic techniques with electrophysiology, we show that BK channels contribute to synaptic currents in high-frequency OHCs of the cochlea. Morphological investigation further revealed altered structure of efferent synapses onto OHCs lacking BK channels.

BK channels have long been known to play a role in regulating presynaptic excitability and transmitter release through their activation by voltage-gated calcium influx (Robitaille and Charlton, 1992; Wang, 2008; Zorrilla de San Martín et al., 2010). The present work examining efferent synapses onto OHCs provides the first direct evidence that BK channels can be functionally coupled to ligand-gated receptors to cause rapid postsynaptic inhibition. Moreover, the presence of BK channels appears essential to the morphological and physiological maturation of these synapses.

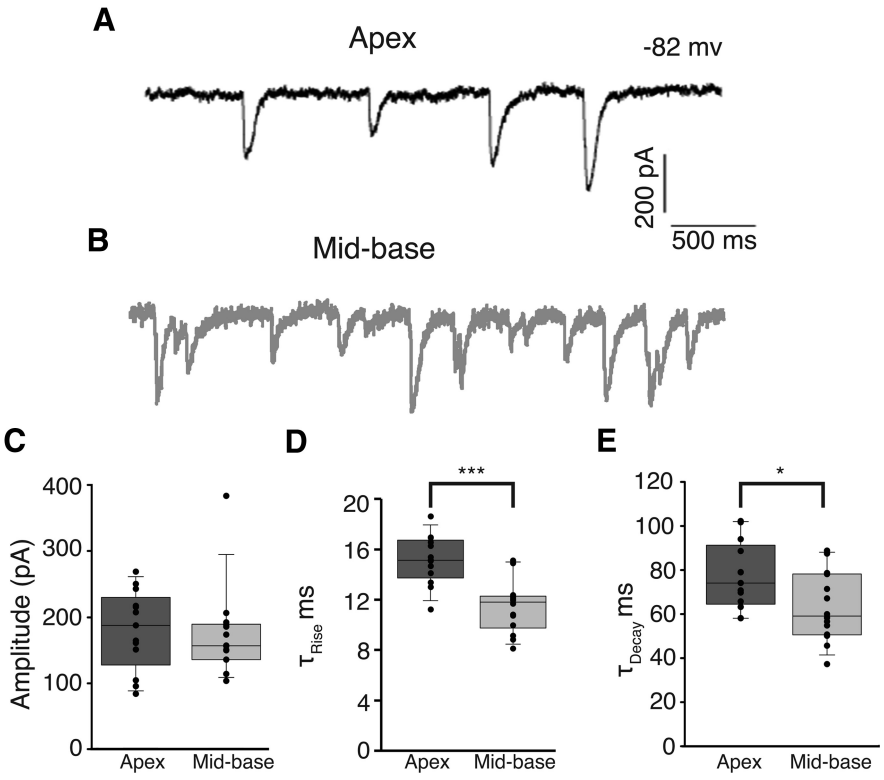

Figure 1. IPSCs in apical OHCs and mid-basal OHCs. Representative traces of 40 mM KCl-induced IPSCs recorded from apical (black, ***A***) and mid-basal (gray, ***B***) cochlear segments from P21 rats. IPSC amplitudes (***C***) were not significantly different between apical and mid-basal cochlear segments. IPSC rise times (***D***) were significantly slower in apical OHCs compared with those recorded from mid-basal OHCs. Likewise, IPSC decay times (***E***) were significantly slower in apical compared with those recorded in mid-basal OHCs. ***C–E***, Dots indicate mean value for each cell within each group. Boxes mark the 25th (closest to zero) and 75th percentiles with a line between marking median value. Whiskers (error bars) above and below the box indicate 10th and 90th percentiles.

Materials and Methods

Animal procedures and tissue preparation

All animal protocols were approved by the Johns Hopkins University and the University of North Carolina at Wilmington Institutional Animal Care and Use Committees. Sprague Dawley rats of either sex aged P10, P14, and P21 were used in experiments involving electrophysiology and immunofluorescence on excised organ of Corti segments. Rats were overdosed with an inhalant anesthetic (isoflurane; Sigma-Aldrich) and killed by decapitation. Tissue was dissected in external solution (see below) maintained at 4°C before electrophysiological recordings or PBS maintained at 4°C before immunofluorescence experiments. For each cochlea, the bone was entirely removed to expose the organ of Corti.

Heterozygous mice with a targeted deletion of the pore-forming BK channel α-subunit were obtained (Meredith et al., 2004) and maintained on the FVB/NJ background used in other studies of auditory function in this same knock-out line and genetic background (Pyott et al., 2007; Maison et al., 2013). Heterozygous offspring were bred to obtain BK$\alpha^{+/+}$ and BK$\alpha^{-/-}$ littermates for experiments at ages P20–P24. The same killing and dissection methods were used as described for rats. All recordings were performed and analyzed blind to the genotype.

Electrophysiology

Rats. Whole-cell, tight-seal voltage-clamp recordings from all rows of OHCs were made immediately after the cochlear dissection. Two tonotopic regions of the rat organ of Corti were examined: the apex, or low-frequency region corresponding to 1–3 kHz, and a mid-base, or high-frequency region between 20 and 40 kHz (Müller, 1991). The extracellular solution contained the following (in mM): 5.8 KCl, 144 NaCl, 0.9 $MgCl_2$, 1.3 $CaCl_2$, 0.7 NaH_2PO_4, 10 HEPES, and 5 glucose, pH 7.4 and 300 mOsm. The recording pipette's solution contained the following (in mM): 120 K-gluconate, 20 KCl, 5 EGTA, 5 HEPES, 2.5 Na_2ATP, 0.1 Ca^{2+}, 3.5 $MgCl_2$, and 10 Na-phosphocreatine, pH 7.2 and 285 mOsm. Currents were recorded at room temperature (22–25°C) using a Multiclamp 700B amplifier and pClamp 10.2 software (Molecular Devices), digitized at 10–20 kHz (Digidata 1440A), and low-pass filtered at 5–10 kHz. Series resistances (typically 7–15 MΩ) were compensated up to 50% on-line. The indicated holding potentials are corrected for a measured 11 mV liquid junction potential.

Since spontaneous IPSCs were extremely rare in control extracellular solution, transmitter release from efferent synapses was accelerated with 40 mM potassium extracellular solution applied by a bath perfusion system (rate flow 3 ml/min). For a subset of apical and mid-basal P21 OHC recordings, baseline 40 mM KCl-evoked IPSCs were followed by application of 40 mM KCl with SK or BK channel antagonists. All drugs (from Tocris Bioscience except apamin from Sigma-Aldrich) were added to the extracellular solution and applied through the bath-perfusion system. Synaptic waveforms were analyzed using Mini Analysis (Synaptosoft). Peak amplitude, 10–90% rise time, and 100% decay time were recorded for each event. In the case of pharmacological experiments, pairwise comparisons were made for IPSCs during predrug (control) and postdrug application for each cell. All rat hair cell recordings are reported as the group average of the means for each cell in the given group. These data are presented as boxplots with superimposed dots indicating individual cell means.

Mice. Whole-cell, tight-seal recordings were made from the first two rows of OHCs of mouse cochleae dissected in the same extracellular solution as used for rats. Because BK immunofluorescence has been reported in all but the very apical tip of the mouse cochlea (Maison et al., 2013), a single tonotopic region corresponding to 6–12 kHz (90–70%) of the mouse organ of Corti (Müller et al., 2005) was examined. The recording pipette solution contained the following (in mM): 135 KCl, 3.5 $MgCl_2$, 0.1 $CaCl_2$, 5 EGTA, 5 HEPES, and 2.5 Na_2ATP. Recordings were done at room temperature (22–25°C) using an Axopatch 200B amplifier and pClamp 9.2 software (Molecular Devices), digitized at 10 kHz (Digi-

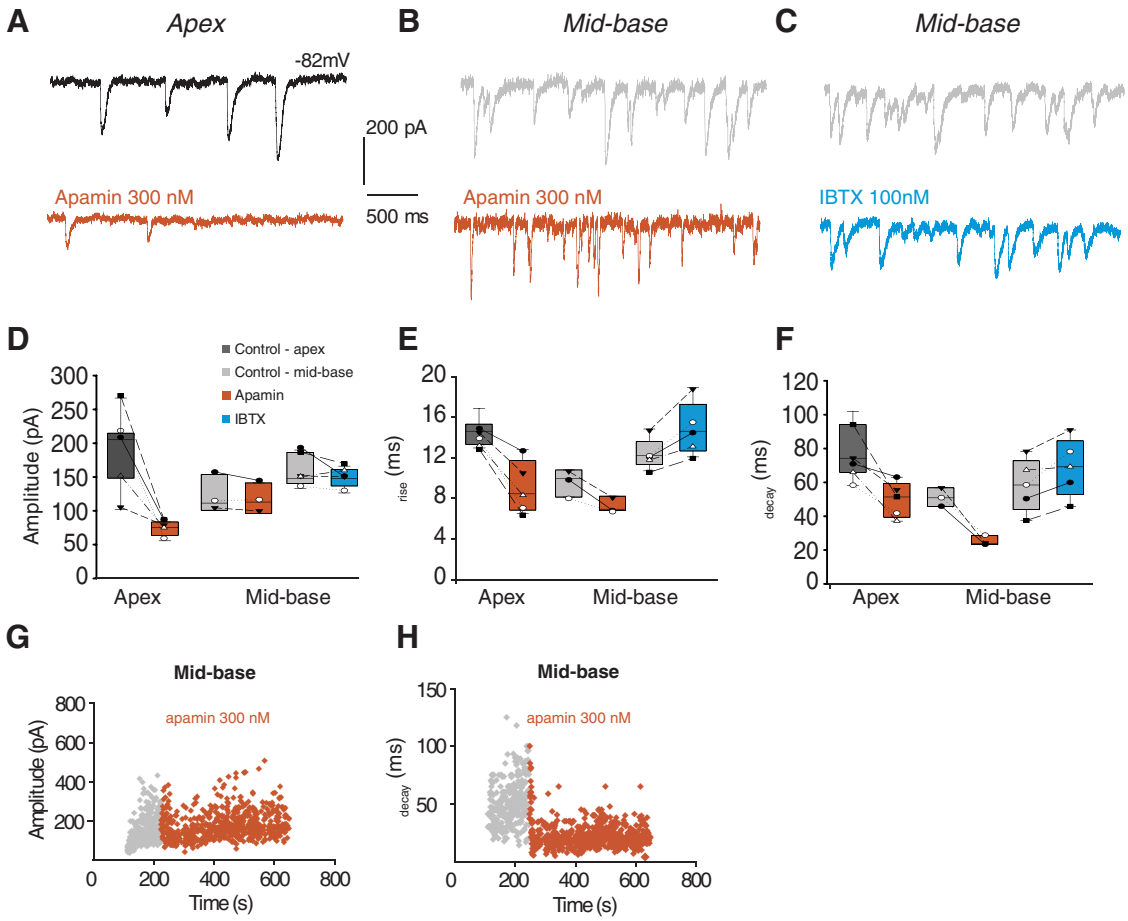

Figure 2. Blockade of SK or BK channels alters IPSCs from apical and mid-basal OHCs. Representative traces of 40 mM KCl-induced IPSCs in apical (***A***, black) or mid-base (***B***, ***C***, gray) OHCs in control extracellular solution and in the presence of 300 nM apamin (red) or 100 nM IBTX (blue). All cochlear segments were from P21 rats. ***D–F***, Data plotted both as group boxplots as well as within-subject measures with individual cell means plotted both before (control) and after pharmacological treatment. Application of 300 nM apamin (red) causes a significant decrease in the amplitude of IPSCs recorded from apical OHCs (***D***). Neither toxin significantly altered IPSC amplitude in mid-basal OHCs (***D***); 300 nM apamin (red) decreased rise (***E***) and decay time (***F***) of IPSCs recorded from either apical or mid-basal OHCs. In contrast, 100 nM IBTX (blue) increased the rise and decay times of IPSCs in mid-basal OHCs. Diary plots of IPSC amplitude (***G***) and decay time (***H***) from mid-basal OHCs before (gray) and after (red) wash-in of 300 nM apamin.

data 1322A), and low-pass filtered at 5 kHz. The indicated holding potentials were not corrected for a measured 4.2 mV liquid junction potential.

Even in 40 mM potassium extracellular solution, the probability of observing IPSCs in mouse OHCs was rare. To increase efferent release, external $CaCl_2$ concentration was increased to 5 mM along with the addition of 3 μM nifedipine, both of which have been shown to enhance efferent synaptic transmission onto immature inner hair cells (Zorrilla de San Martín et al., 2010). Measurements and analyses were performed as described for rats. Reported means are the average of all IPSCs recorded from multiple OHCs of a given genotype. These data are presented as boxplot distributions of the entire IPSC dataset for all events across multiple cells.

Immunofluorescence, light microscopy, and image analysis

Immunofluorescent staining was performed as described previously (Wersinger et al., 2010) using a mouse monoclonal anti-BK (L6/43 1:300; University of California Davis/NIH NeuroMab Facility), a rabbit polyclonal anti-synapsin I (AB1543sc-136237; 1:600; EMD Millipore), and the appropriate secondary antibodies (goat anti-rabbit and goat anti-mouse Alexa Fluor 488 and Alexa 594; 1:500; EMD Millipore). Micrographs were acquired using an Olympus FluoView FV1000 confocal microscope with either a 10× air or 60× oil-immersion lens under the control of the Olympus FluoView FV10-ASW 2.1 software (Olympus Corporation). Tonotopic maps were superimposed on low-magnification micrographs of complete organs of Corti in ImageJ (Müller, 1991, 2005). High-magnification confocal micrographs of identified tonotopic regions were collected to encompass the entire synaptic pole of all three rows of OHCs. BK immunopuncta volumes were measured from 3D reconstructions generated using Imaris 6.4 (Bitplane). Because detection of synapsin-positive efferent terminals in 3D reconstructions was highly variable, especially at P12, the sizes of the synapsin-positive efferent terminals were determined instead from the surface areas of flattened *z*-projections. Surface areas were identified and measured in ImageJ after converting the flattened images to binary (black and white) images.

Electron microscopy and image analysis

The otic capsules from deeply anesthetized mice were opened at the apex and fixative containing 1% osmium (OsO4) and 1% potassium ferricyanide [FeK3(CN)6] in 0.1 M sym-collidine-HCl buffer, pH 7.4, was perfused through the round window. The tissue was postfixed for1 h, rinsed with 0.1 M maleate buffer, pH 7.4, and decalcified with agitation for 48–72 h at 40°C in 5% EDTA in 0.1 M phosphate buffer (pH 7.4–7.8). Then the cochleae were processed for embedding into Araldite. Sections (40 μm thick) were cut parallel to the cochlear modiolus, then re-embedded in Epon sandwiched between Aclar sheets (EMS). Photographs were taken of organ of Corti segments selected for thin sections.

The selected segments were remounted onto Epon blocks for ultrathin sectioning (Leica Ultracut S) perpendicular to the organ of Corti so that each image showed inner and outer hair cell rows in cross section. Serial 65-nm-thick sections were collected onto Formvar-coated slot grids for examination on a Hitachi H7600 TEM at 80 kV.

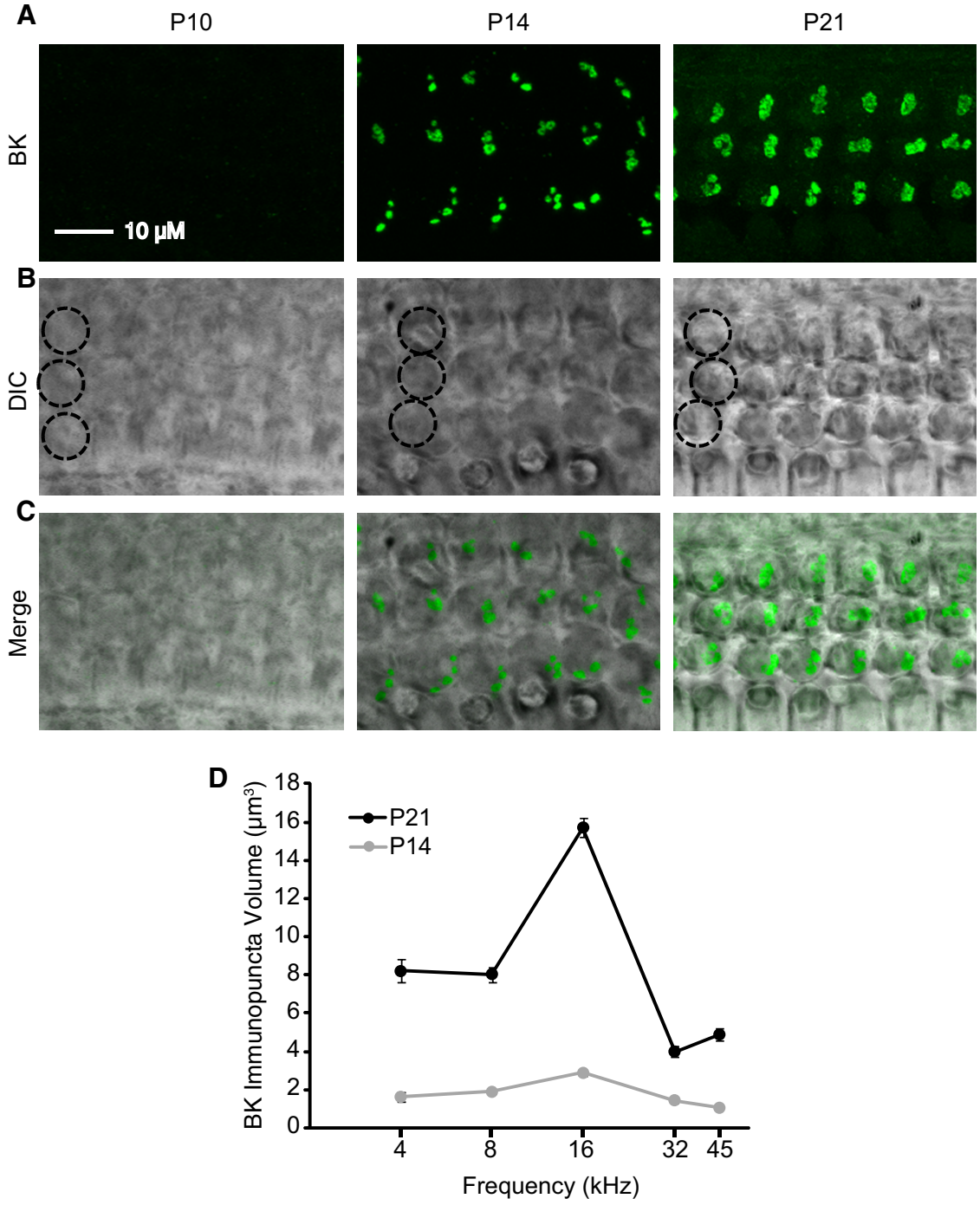

Figure 3. Expression of BK channels at efferent synapses onto mid-basal OHCs at P10 and P14. BK channel immunoreactivity in OHCs was quantified in five tonotopic regions (4, 8, 16, 32, and 45 kHz) at P10, P14, and P21. ***A***, Z-projections of stacks of confocal images spanning the OHC region containing BK channel immunoreactivity (green). ***B***, DIC micrographs of the corresponding regions with a single column of three OHCs circled. ***C***, Overlay of fluorescent and DIC images. ***A–C***, All micrographs and projections taken from the 16 kHz region. ***D***, Volume of BK channel immunopuncta plotted as a function of age and tonotopic position. No BK channel immunoreactivity was observed at P10. No BK channel immunoreactivity in regions <3 kHz was observed at either P14 or P21.

Table 1. BK channel immunopuncta volume (μm^3) as a function of developmental age and tonotopic location

Frequency (kHz)	P14 Mean ± SEM	*N* (immunopuncta from at least three animals)	P21 Mean ± SEM	*N* (immunopuncta from at least three animals)
4	1.63 ± 0.25	51	8.20 ± 0.60	135
8	1.90 ± 0.09	395	8.05 ± 0.39	271
16	2.89 ± 0.15	262	15.71 ± 0.49	205
32	1.46 ± 0.11	160	4.00 ± 0.29	137
45	1.06 ± 0.07	118	4.89 ± 0.34	88

Identified efferent synapses were photographed in consecutive serial sections. Digital images (2120 × 2120 pixels) were recorded at 8-bit or 16-bit depth.

Synaptic images were collected at magnifications of 30,000–100,000. Serial images were imported into Reconstruct (Fiala, 2005) for alignment, calibration, and 3D reconstruction. In each image the outline of hair cells, postsynaptic cisterns, and synaptic contacts was traced. The volumes of the synaptic cistern and the underlying cytoplasmic gap were computed based on a nominal section thickness of 65 nm. The *z*-axis areas of efferent terminals and synaptic cisterns were obtained by tracing their extent

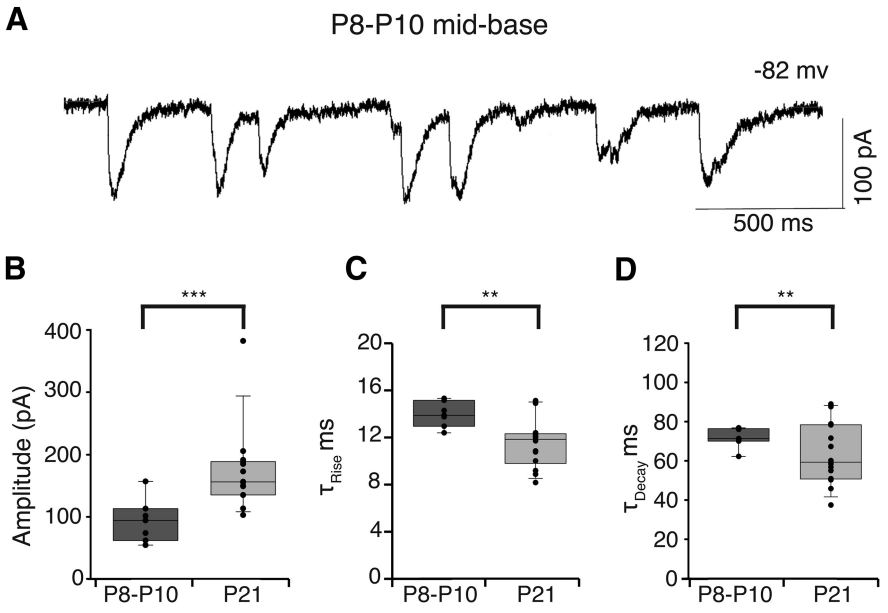

Figure 4. IPSCs from immature mid-basal OHCs. Representative trace of 40 mM KCl-induced IPSCs recorded from P10 mid-basal OHC (***A***). IPSCs were significantly smaller than those from mid-basal OHCs at P21 (***$p < 0.0001$; ***B***). Rise (***C***) and decay times (***D***) of IPSCs were significantly slower than those of P21 mid-basal OHCs (**$p < 0.01$). ***B–D***, Dots indicate mean value for each cell within each group.

in each section, multiplying by the section thickness, and then summing for all sections in the series. This *z*-axis area was divided into the 3D volume to obtain the average width of the cisternal lumen and underlying cytoplasmic gap.

Statistical analyses

Group results are reported as the mean ± SEM. Statistical analyses were performed using GraphPad Prism 4. For rat OHC physiology, a normality test was performed to verify the Gaussian distribution of data before performing Student's *t* test to compare the means (using an α-level set to 0.05). Unpaired *t* tests were used for rat physiology except in the case of pharmacology experiments in which paired *t* tests were applied before (control) and after drug application IPSC measures. For BK knock-out physiology where IPSC data did not conform to a Gaussian distribution, an unpaired *t* test with Welch's correction was performed. For immunofluorescence experiments, a Kruskal–Wallis test followed by a Dunn's multiple-comparison test was used to determine statistically significant differences between the five frequencies and two age groups examined to investigate tonotopic and developmental differences in BK channel expression in rat and also the two developmental and two genotype groups examined to investigate the role of BK channels in the morphological maturation of efferent presynaptic terminals in mice. Statistical significance for EM reconstructions was established by two-tailed unpaired *t* test.

Results

IPSCs from apical OHCs have slower time courses than IPSCs from mid-basal OHCs

Whole-cell, tight-seal intracellular recordings were made from OHCs in apical and mid-basal cochlear segments isolated from the inner ear of P21 rats as reported previously (Wersinger et al., 2010). Synaptic release of ACh from efferent terminals was driven by potassium depolarization (40 mM). OHCs were voltage clamped to −82 mV so that synaptic currents were entirely inward in the high-potassium condition and included a combination of cation current through AChRs and potassium current through associated calcium-dependent potassium channels. Under these conditions IPSCs were observed in ~50% of apical (17/30) or mid-basal (9/20) OHCs at P21. IPSCs in apical and mid-basal OHCs were not significantly different in amplitude and averaged 175 pA ($p = 0.272$; unpaired *t* test; Fig. 1*C*). In contrast, IPSC rise times were significantly slower in apical OHCs (15.1 ± 0.5 ms, $n = 13$ OHCs) compared with basal OHCs (11.4 ± 0.6 ms, $n = 14$ OHCs, $p < 0.0001$; unpaired *t* test; Fig. 1*D*). Likewise, IPSC decay times were significantly slower in apical (77.4 ± 4.3 ms, $n = 13$ OHCs) compared with basal OHCs (63.4 ± 4.2 ms, $n = 14$ OHCs, $p < 0.05$; unpaired *t* test; Fig. 1*E*). The supposition to be tested is that these differences in waveform result from the gating kinetics of the associated calcium-dependent potassium channels.

Blockade of either SK2 or BK calcium-activated potassium channels alters the time course of IPSCs in OHCs

Previous work has shown that BK channels expressed by mid-basal OHCs can be activated by exogenous ACh (Wersinger et al., 2010). Under the present recording conditions (V_m −82 mV, E_K ~−40 mV), potassium current is inward and dominates the synaptic waveform. Thus, the briefer IPSCs of mid-basal OHCs could reflect the participation of rapidly gating BK channels. To test this possibility, blockers specific to either SK channels (apamin) or BK channels (iberiotoxin, IBTX) were applied to a subset of the apical and mid-basal OHCs included in Figure 1 and the effects on synaptic waveform were measured. Representative recordings in control extracellular solution (black) and with either 300 nM apamin (red) or 100 nM IBTX (blue) suggest that either toxin can alter the appearance of IPSCs, depending on cochlear location of the OHC (Fig. 2). To compare toxin effects across multiple cells, individual IPSC waveforms were measured and averaged before and during the period of toxin exposure (Fig. 2*D–F*). Application of 300 nM apamin caused a significant reduction (from 188.4 ± 20.3 to 75.5 ± 5.1; $n = 7$ OHCs; $p < 0.05$; paired *t* test) in IPSC amplitude in apical OHCs, as previously reported in outer and inner hair cells (Glowatzki and Fuchs, 2000; Oliver et al., 2000; Katz et al., 2004). The residual IPSC rose and fell faster after exposure to apamin (Fig. 2*E*,*F*), consistent with the observation that SK gating kinetics are slower than the underlying calcium influx through the hair cell's AChR (Oliver et al., 2000; Katz et al., 2004). Apamin (300 nM) reduced both the rise (from 14.6 ± 0.5 to 9.1 ± 1.2 ms; $p < 0.05$; paired *t* test) and decay time (from 77.8 ± 5.8 to 49.8 ± 4.7 ms; $p < 0.05$; paired *t* test) of IPSCs in apical OHCs, indicating that inward potassium current is substantially larger than cation flux through the AChR, and so dominates both rising and falling phases.

However, neither apamin nor IBTX on its own significantly altered IPSC amplitude in mid-basal OHCs (Fig. 2*D*). Application of 300 nM apamin (Fig. 2*G*) produced a nonsignificant reduction of IPSC amplitude (average control amplitude 123.3 ± 16.1 and 118.2 ± 13.1 pA in apamin, $n = 3$ OHCs). IBTX (100 nM) caused a slightly greater, but still nonsignificant reduction of the average IPSC amplitude (control 166.5 ± 10.7 and 149.9 ± 6.5 pA in IBTX; $n = 5$ OHCs). However, IPSC time course in mid-basal OHCs was significantly altered by exposure to SK or BK channel blockers (Fig. 2*E*,*F*,*H*). Application of 300 nM apamin reduced the rise time (from 11.6 ± 0.8 to 7.3 ± 0.4 ms; $p < 0.05$; paired *t* test) in mid-basal OHCs. Apamin also reduced

IPSC decay time in mid-basal OHCs (from 51.1 ± 3.2 to 25.3 ± 1.7 ms; $p < 0.01$; paired t test; Fig. 2*H*). In contrast, 100 nM IBTX had the opposite effect on IPSC kinetics in mid-basal OHCs. The BK channel blocker significantly increased both the rise time (from 12.4 ± 0.7 to 14.9 ± 1.2 ms; $p < 0.05$; paired t test) and the decay time (from 58.3 ± 7.0 to 68.8 ± 7.7 ms; $p < 0.05$; paired t test). These results suggest that blockade of rapidly gating BK channels with IBTX leaves only slowly gating SK channels to shape the time course of IPSCs in mid-basal OHCs.

BK channel expression occurs several days after efferent contacts form on mid-basal OHCs

As an alternative strategy to evaluate the contribution of BK channels to efferent synaptic currents, the developmental appearance of BK channel immunoreactivity in OHCs was charted in five tonotopic regions (4, 8, 16, 32, and 45 kHz; Fig. 3, Table 1) defined using maps determined for juvenile rats (Müller, 1991). Example micrographs from the 16 kHz region of the organ of Corti are displayed as flattened z-projections with BK channel immunoreactivity (Fig. 3*A*,*C*, green) overlaid on differential interference contrast micrographs (Fig. 3*B*,*C*) to show the locations of the OHCs. As reported previously (Wersinger et al., 2010), no BK channel immunoreactivity was associated with OHCs in P10 rats at any of the tonotopic regions examined (Fig. 3*A*). By P14, BK channel immunoreactivity was present in OHCs at all tonotopic regions examined (Fig. 3*D*), with significantly greater expression in the 8 and 16 kHz regions compared with the 4, 32, and 45 kHz regions ($p < 0.01$). By P21, BK channel immunoreactivity (Fig. 3*D*) increased significantly in all tonotopic regions compared with values at P14 ($p < 0.0001$). Moreover, by P21, BK channel immunoreactivity was significantly greater in the 16 kHz region compared with all other tonotopic regions at this age ($p < 0.0001$), suggesting that the tonotopic pattern in BK channel expression, as reported previously in 6-week-old mice (Maison et al., 2013), is established in rats by the third postnatal week. Summary statistics are provided in Table 1. Importantly, no BK channel immunoreactivity was observed in OHCs from the most apical regions (<3 kHz) at any age. Thus, BK channels appear relatively late during OHC maturation in the rat, akin to the pattern observed in mouse inner hair cells (Pyott et al., 2004; Hafidi et al., 2005) and in hair cells of the chicken basilar papilla (Fuchs and Sokolowski, 1990). Rat hair cells show no BK expression in the most apical tonotopic regions, and peak in expression in the 16 kHz region as observed in mouse OHCs (Maison et al., 2013).

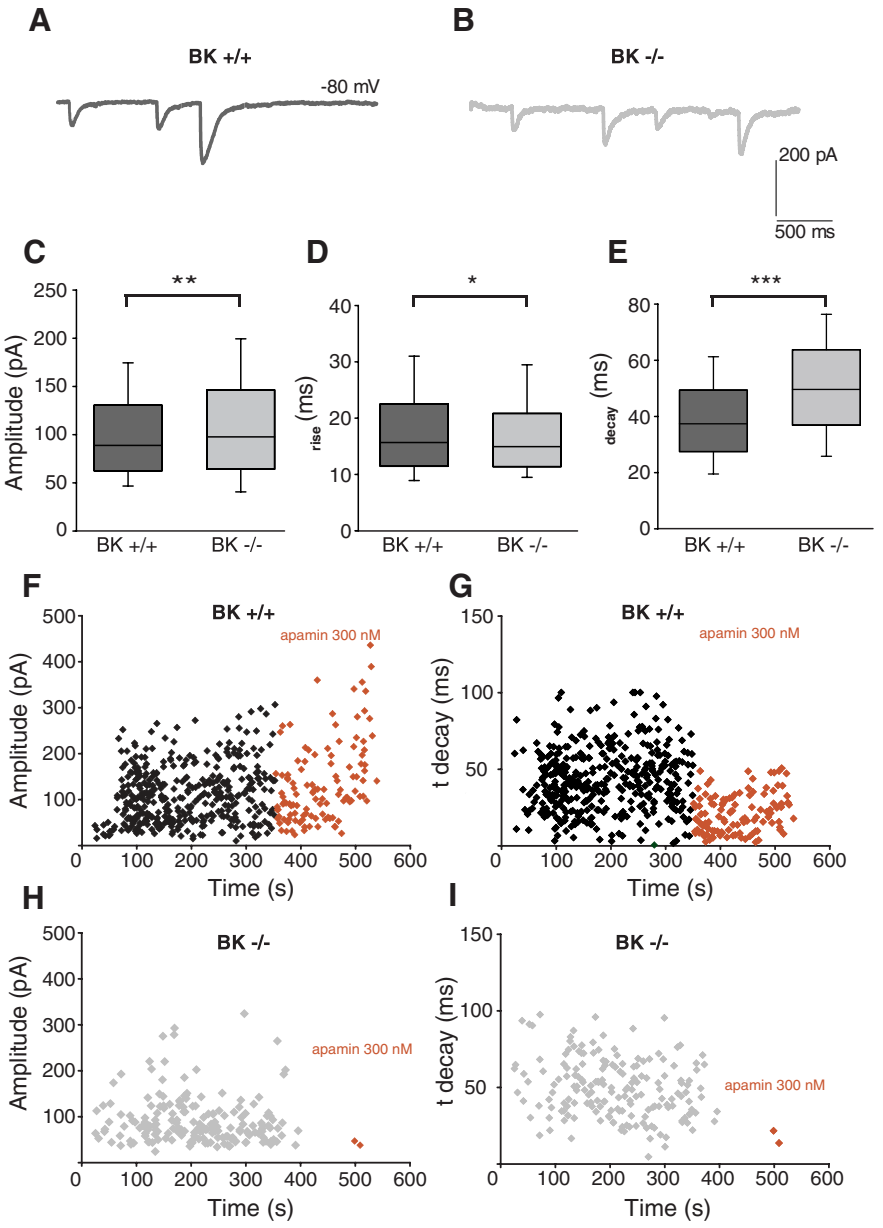

Figure 5. IPSCs in OHCs from P20–P24 BK$\alpha^{+/+}$ and BK$\alpha^{-/-}$ mice. Representative traces of 40 mM KCl-induced IPSCs recorded from mid-apical OHCs of BKα+/+ (***A***) and BK$\alpha^{-/-}$ mice (***B***). There were significant effects of genotype on amplitude (***C***; $^{**}p < 0.01$), 10–90 rise time (***D***; $^{*}p < 0.05$), and decay time (***E***; $^{***}p < 0.0001$) of 40 mM KCl-induced IPSCs. Diary plots of IPSC amplitude (***F***, ***H***) and decay time (***G***, ***I***) in BKα+/+ (***F***, ***G***) and BK$\alpha^{-/-}$ (***H***, ***I***) mouse mid-apical OHCs before and during exposure to 300 nM apamin.

Slower IPSCs in immature mid-basal OHCs

Given that BK channels appear later during development (>P10, see above) than the efferent endings contacting mid-basal OHCs (as early as P8; Roux et al., 2011), the IPSC time course may show changes commensurate with the developmental acquisition of these rapidly gating channels. Indeed, smaller and slower potassium-evoked IPSCs could be observed in mid-basal OHCs as early as P8 (Fig. 4*A*). The average IPSC amplitude from P8–P10 mid-basal OHCs was half (93.0 ± 13.2 pA; $n = 705$ IPSCs from 7 OHCs; Fig. 4*B*) that at P21 (174.2 ± 17.9 pA, $p < 0.0001$; unpaired t test; from Fig. 1). The average IPSC rise time in P8–P10 mid-basal OHCs was significantly slower (13.9 ± 0.4 ms; Fig. 4*C*) than that from P21 mid-basal OHCs (11.8 ± 0.6 ms, $p < 0.01$; unpaired t test;

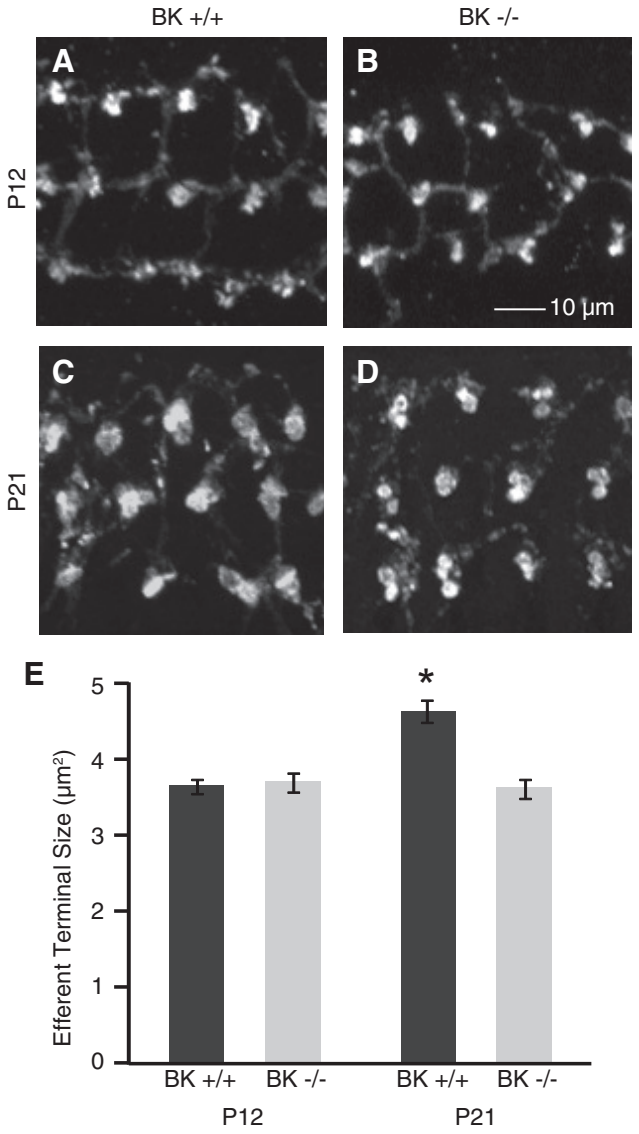

Figure 6. Medial olivocochlear (MOC) efferent presynaptic terminals in BK$\alpha^{+/+}$ and BK$\alpha^{-/-}$ mice. MOC efferent presynaptic terminals from the 16 kHz region were identified by synapsin immunoreactivity in BKα+/+ and BK$\alpha^{-/-}$ mice aged P12 and P21. ***A–D***, Example micrographs are displayed as flattened *z*-projections. ***E***, Efferent terminal sizes were calculated from the surface areas of immunoreactive areas in the flattened *z*-projections and were significantly smaller in P12 BKα+/+ and BK$\alpha^{-/-}$ mice as well as P21 BK$\alpha^{-/-}$ mice compared with P21 BKα+/+ mice (*$p < 0.0001$).

Fig. 1). Likewise, the average decay time of IPSCs in P8–P10 mid-basal OHCs was significantly slower (72.0 ± 1.9 ms; Fig. 4*D*) than that from P21 mid-basal OHCs (63.4 ± 4.2 ms, $p < 0.01$; unpaired *t* test; Fig. 1). Thus, IPSCs in basal OHCs become larger and faster during the second and third postnatal weeks, in parallel with the developmental arrival of BK channels as documented by immunofluorescence.

IPSCs in OHCs of BK channel knock-out and wild-type mice

The pore-forming α-subunit of BK channels in cochlear hair cells is encoded by the KCNMA1 gene whose removal of exon 1 results in a knock-out mutation, eliminating membrane currents carried by these channels (Rüttiger et al., 2004; Pyott et al., 2007; Kurt et al., 2012). OHCs and efferent innervation remain intact for at least the first 2–3 months in the null mice (Maison et al., 2013), providing an opportunity to examine synaptic function in the absence of this channel. Therefore, intracellular recordings were made from OHCs in excised mid-apical cochlear turns of homozygous BK$\alpha^{-/-}$ knock-out mice and BK$\alpha^{+/+}$ wild-type littermates. The current–voltage curve (10 mV steps from −100 to 50 mV) was recorded from each OHC before application of high-potassium extracellular solution to elicit transmitter release from the efferent terminals. Voltage-gated currents were not extensively analyzed; however, there was no significant difference in maximum evoked currents (at + 50 mV) between genotypes (BK$\alpha^{+/+}$: 5.6 ± 1.5 nA, $n = 13$ cells; BK$\alpha^{-/-}$: 5.7 ± 9.4 nA, $n = 11$ cells; $p = 0.98$; unpaired *t* test).

IPSCs were recorded from a total of six BK$\alpha^{+/+}$ and 5 BK$\alpha^{-/-}$ OHCs. The 40 mM extracellular potassium evoked IPSCs (Fig. 5*A*,*B*; sample traces) that differed in amplitude (BK$\alpha^{+/+}$:101.7 ± 1.4 pA, $n = 1502$ IPSCs; BK$\alpha^{-/-}$ 110.1 ± 2.2, $n = 804$ IPSCs, $p < 0.001$; unpaired *t* test; Fig. 5*C*), 10–90 rise time (BK$\alpha^{+/+}$ 18.29 ± 0.25 ms, $n = 1502$ IPSCS; BK$\alpha^{-/-}$ 17.38 ± 0.30, $n = 804$ IPSCs, $p = 0.019$; unpaired *t* test; Fig. 5*D*), and decay time (BK$\alpha^{+/+}$ 39.41 ± 0.44 ms, $n = 1502$ IPSCs; BK$\alpha^{-/-}$ 50.67 ± 0.68, $n = 804$ IPSCs, $p < 0.0001$; unpaired *t* test; Fig. 5*E*). Across all three measures, there were significant differences between genotypes; however, these differences were small save for decay time. Exposure to the SK blocker apamin (300 nm) reduced the average amplitude (214.23 vs 134.33 nA; Fig. 5*F*) and decay time (79 vs 21.43 ms; Fig. 5*G*) of IPSCs in mid-apical BK$\alpha^{+/+}$ OHC. This is similar to results from rat apical OHCs exposed to 300 nm apamin (Fig. 2*D*,*F–H*) and confirms the participation of SK channels in efferent inhibition of mouse OHCs. Only one OHC tested with apamin proved to be from a BK$\alpha^{-/-}$ mouse in these blinded recordings. Exposure to 300 nm apamin in BK$\alpha^{-/-}$ OHC all but abolished IPSCs (Fig. 5*H*) and shortened decay time (Fig. 5*I*) leaving just two rapidly decaying synaptic events in this OHC.

Efferent synaptic structure in OHCs of BK channel wild-type and knock-out mice

A previous study found that efferent terminals, identified by vesicular acetylcholine transporter immunoreactivity, on OHCs were slightly smaller throughout most tonotopic regions of BK$\alpha^{-/-}$ compared with BK$\alpha^{+/+}$ mice aged 6–9 weeks (Maison et al., 2013). Efferent terminals in younger mice were similarly examined to match the age at which these physiological studies were performed and also to investigate the developmental role of the BK channel in their maturation. Specifically, efferent presynaptic terminals from the 16 kHz region were identified by synapsin immunoreactivity in BK$\alpha^{+/+}$ and BK$\alpha^{-/-}$ mice aged P12 (just before the onset of BK channel expression) and P21 (Fig. 6*A–D*). Organs of Corti from P12 mice were immunolabeled with an antibody against the BK channel to verify the lack of channel expression at this age and tonotopic region (data not shown). Efferent terminals analyzed as immunoreactive areas of flattened *z*-projections (Fig. 6*E*) were significantly smaller in immature (P12) BK$\alpha^{+/+}$ (3.63 ± 0.09 μm^2; $n = 496$ immunopuncta from three animals), BK$\alpha^{-/-}$ mice (3.68 ± 0.12 μm^2; $n = 341$ immunopuncta from three animals), and P21 BK$\alpha^{-/-}$ mice (3.60 ± 0.12 μm^2; $n = 201$ immunopuncta from three animals) compared withP21 BK$\alpha^{+/+}$ mice (4.62 ± 0.15 μm^2; $n = 179$ immunopuncta from three animals; $p < 0.0001$). Thus, efferent presynaptic terminals onto OHCs are smaller in BK$\alpha^{-/-}$ mice already at 3 weeks of age, perhaps because they retain their immature (reduced) size in the developmental absence of the BK channel.

Genetic knock-out of the SK channel eliminates cholinergic sensitivity and severely disrupts efferent innervation of OHCs (Kong et al., 2008; Murthy et al., 2009), greatly reducing the size and number of postsynaptic cisterns (Fuchs et al., 2014). It was of interest then to determine whether postsynaptic ultrastructure remained normal in BK$\alpha^{-/-}$ OHCs. Serial section electron microscopy (Fig. 7*A*,*B*) was performed to characterize the cisterns in OHCs of BK$\alpha^{+/+}$ and littermate BK$\alpha^{-/-}$ mice. In each image the efferent contacts and hair cell membranes were traced. The synaptic cistern and the cytoplasmic space lying between the cistern and the plasma membrane were outlined. From these tracings the 3D volume of the cistern and the underlying cytoplasmic gap were computed (Fig. 7*C*,*D*). In addition, the *z*-axis contact area of the efferent terminal and that of the synaptic cistern with the hair cell membrane was determined. The ratio of the cistern to efferent contact area indicates the degree of overlap between these presynaptic and postsynaptic specializations. In a subset of synapses, the average lumenal thickness of the synaptic cistern and that of the underlying cytoplasmic gap were obtained by dividing their 3D volume by the *z*-axis appositional area for each. The average width of the cytoplasmic gap (the distance between the hair cell plasma membrane and the cisternal membrane) in 7 BK$\alpha^{+/+}$ synapses was 15.0 ± 2.0 nm, and was 14.9 ± 1.4 nm for 22 BK$\alpha^{-/-}$ synapses, not different from that found for other mouse lines (Fuchs et al., 2014). The average cisternal lumen was 16.3 ± 2.2 nm in BK$\alpha^{+/+}$ mice and 16.6 ± 0.1 nm in BK$\alpha^{-/-}$ OHCs, so that the cistern to gap volume ratio (1.1–1.2) was slightly smaller than that found in other mouse lines (1.3; Fuchs et al., 2014).

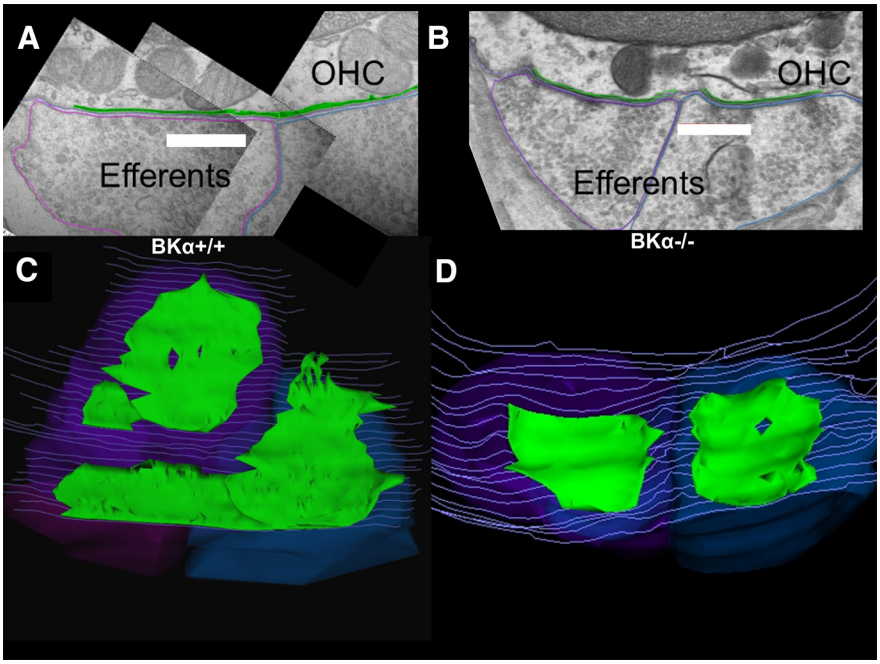

Figure 7. Ultrastructure of efferent synapses in BK$\alpha^{+/+}$ and BK$\alpha^{-/-}$ mice. ***A***, Cross section showing vesicle-rich efferent terminals contacting an OHC in the basal cochlea of wild-type mouse. The synaptic cisterns are outlined in green, efferent terminals in purple and blue, and hair cell membrane in gray. Scale bar, 500 nm. ***B***, Cross section of two efferent contacts on an OHC in the basal cochlea of a BK$\alpha^{-/-}$ mouse. Cisterns outlined in green and efferent terminals in purple and blue. Scale bar, 500 nm. ***C***, *Z*-axis projection (tilted ~45 degrees forward from plane of section) of 3D reconstruction of 37 serial sections including that in ***A***. ***D***, *Z*-axis projection (tilted ~30 degrees forward from plane of section) of 3D reconstruction of 21 serial sections including that in ***B***.

Synaptic cisterns are co-extensive with efferent terminals in OHCs of other mouse lines; i.e., the ratio of appositional area of the cistern to the terminal is close to 1 (Fuchs et al., 2014). Likewise in BK$\alpha^{+/+}$ OHCs the appositional area of the synaptic cistern was nearly co-extensive with the efferent terminal, averaging 0.85 ± 0.14 for 26 synapses on 10 OHCs from two wild-type mice. In the BK$\alpha^{-/-}$ OHCs, however, the cisterns were smaller in extent than the associated efferent terminal, with an average appositional ratio of 0.67 ± 0.15 for 23 synapses on 15 OHCs in 2 BK$\alpha^{-/-}$ mice. This was significantly different from the area ratio of wild-type synapses (p = 0.01, two-tailed t test). Finally, immunolabeling showed that the contact area of efferent terminals was smaller on BK$\alpha^{-/-}$ OHCs than on those of wild-type littermates (Fig. 6). The electron micrographs suggest that this results both from smaller and fewer terminals contacting BK$\alpha^{-/-}$ OHCs (1.53 ± 0.61 terminals on 15 BK$\alpha^{-/-}$ OHCs; 2.66 ± 1.49 terminals on 10 BK$\alpha^{+/+}$ OHCs, p = 0.07, two-tailed t test). Although this difference does not reach significance the trend is consistent with a previous report of fewer efferent terminals on BK$^{-/-}$ OHCs (Maison et al., 2013).

Discussion

Vertebrate hair cells are subject to efferent inhibition through an $\alpha9\alpha10$-containing cholinergic receptor acting together with small conductance (SK) calcium-activated potassium channels (Elgoyhen et al., 2009; Wersinger and Fuchs, 2011). One exception may involve BK channels in type II vestibular hair cells of guinea pig (Kong et al., 2005), although this may result secondarily through activation of voltage-gated calcium channels rather than by direct coupling to the hair cell's AChRs (Kong et al., 2007). The gating kinetics of SK2 channels can account for the waveform of IPSCs in apical OHCs of the rat cochlea (Oliver et al., 2000), and deletion of the SK2 gene severely disrupts efferent synaptic structure and function in mice (Kong et al., 2008; Murthy et al., 2009). In addition, calcium-sensitive BK potassium channels have been proposed to carry voltage-gated current in OHCs (Mammano and Ashmore, 1996) and can be activated by application of ACh as well as by membrane depolarization (Wersinger et al., 2010). The present work demonstrates that BK channels participate directly in the synaptic (efferent) inhibition of OHCs in the higher frequency regions of the mammalian cochlea. Interestingly, BK channels are absent from a longer extent of the rat cochlear apex than seen in mice, perhaps reflecting the extended low-frequency sensitivity of rats compared with mice (Ehret, 1974; Kelly and Masterton, 1977), supporting the hypothesis that BK channel expression is related to functional requirements for higher frequency signaling.

To establish the role of BK channels in efferent inhibition of mammalian OHCs, we compared voltage-clamp recordings of synaptic currents from apical OHCs, which do not express BK channels, to those from basal OHCs, which do express BK channels at the efferent synapse (Wersinger et al., 2010). The prediction was that the faster activation and deactivation kinetics of BK channels revealed their expression by enabling more rapid IPSCs than those resulting from SK gating only. Four main observations support this prediction. First, synaptic waveforms were intrinsically slower in apical OHCs, where SK but no BK channels are found. Second, the IBTX block of BK channels slowed the time

course of IPSCs in mid-basal OHCs, consistent with remaining SK channels dominating the waveform. Third, IPSCs recorded from immature mid-basal OHCs, before the onset of BK channel expression as verified by immunofluorescence, had slower waveforms that were more like those of apical OHCs or of mature mid-basal OHCs in the presence of the BK channel blocker IBTX. Fourth, synaptic waveforms were slower (longer decay time) in OHCs of mice lacking the pore-forming subunit of the BK channel than in OHCs of wild-type littermates.

These conclusions are based on the contribution of BK and SK channels to the decay time of IPSCs where current through associated AChRs does not contribute (Oliver et al., 2000; Katz et al., 2004). In most experiments the presence of BK channels also correlated with larger, more rapidly rising IPSCs. However, these latter measures should be interpreted with caution as they depend on the relative contributions of current through AChRs and potassium channels, which are unknown and could vary between cells. In addition, IPSC amplitude might be influenced by variations in efferent release probability (Ballestero et al., 2011), which itself can be modulated by presynaptic BK channel activity (Zorrilla de San Martín et al., 2010).

The participation of BK channels in efferent inhibition of OHCs specifically in the higher frequency regions of the cochlea raises two questions. First, why are large conductance, faster gating BK channels expressed in high-frequency OHCs? High-frequency OHCs have larger basolateral and mechanotransducer conductances than do apical hair cells (Beurg et al., 2006; Wersinger et al., 2010; Johnson et al., 2011), resulting in much lower input resistance and shorter membrane time constants (Johnson et al., 2011), thus conferring a higher overall frequency response. Incorporation of large conductance, rapidly gating BK channels into efferent inhibition provides a dual benefit. BK channels provide a larger conductance change for a given release of ACh, while more rapid BK gating (submillisecond compared with that of SKs ~6 ms on-rate; Oliver et al., 2000; Fakler and Adelman, 2008) provides better voltage control during rapidly changing receptor potentials. In essence, BK gating should increase the gain and speed of the efferent synaptic "voltage clamp."

The second question to consider is the nature of the postsynaptic calcium signal at efferent synapses. This is of particular interest since BK channel gating typically involves activation by the combination of increased calcium and membrane depolarization—the latter of which does not occur during synaptic inhibition of the hair cell. Coactivation during single IPSCs (stochastic release driven by potassium depolarization) shows that BK and SK channels must colocalize with AChRs in the postsynaptic membrane underlying the synaptic cistern. At this location they adjoin a restricted (<20 nm wide), essentially planar diffusion space formed by the extensively parallel cisternal and plasma membranes (Fuchs et al., 2014). Influx through the hair cell AChRs (Gómez-Casati et al., 2005) should raise calcium to high levels in this subcisternal space, independent of additional calcium that might be released from the synaptic cistern during prolonged activity (Sridhar et al., 1997; Lioudyno et al., 2004). This calcium signal is sufficient to activate SK and BK channels, even without an accompanying depolarization. It will be of interest to learn whether OHC-specific splice variants or accessory subunits (Fettiplace and Fuchs, 1999) underlie this voltage-independent gating of BK channels.

A fully co-extensive postsynaptic cistern that ensures local calcium accumulation may be particularly important for those OHCs that depend on efferent activation of low-affinity BK channels. It is intriguing then that BK$\alpha^{-/-}$ OHCs have smaller cisterns, but whether this has direct functional consequences remains to be determined. A more informative strategy may be to quantify postsynaptic ultrastructure in apical (SK only) versus basal rat OHCs, or in hair cells of other species that employ only SK channels. A recent study found that postsynaptic cisterns covered only half the terminal contact area in chicken hair cells (Im et al., 2014), where cholinergic inhibition is mediated by SK channels (Fuchs and Murrow, 1992; Yuhas and Fuchs, 1999).

Beyond consideration of structure—function relations, potassium channel expression may play a role in synapse formation and maturation. In SK channel-null mice efferent innervation is severely diminished (Murthy et al., 2009), hair cells are insensitive to ACh (Kong et al., 2008), and postsynaptic cisterns are much reduced in size and number (Fuchs et al., 2014). Direct molecular interactions between SK2 and ACh receptors that shuttle ACh receptors to the hair cell membrane may be necessary in mammalian hair cells as in chicken (Scholl et al., 2014). In contrast, OHCs in BK$\alpha^{-/-}$ mice still have functional efferent synapses, although less extensive and with smaller postsynaptic cisterns. SK channel expression is temporally correlated with the onset of efferent synaptic function (Roux et al., 2011) while BK channel expression follows several days later in OHCs. This suggests that, absent the later arrival of BK channels, efferent synapses may fail to differentiate fully and so remain "apical-like" throughout the cochlea. Although SK-mediated efferent inhibition persists in BK$\alpha^{-/-}$ OHCs, efferent suppression of distortion product oto-acoustic emissions is substantially reduced (Maison et al., 2013), emphasizing the specific benefit of larger, more rapidly gating BK channels for efferent inhibition of OHCs.

References

Ballestero J, Zorrilla de San Martin J, Goutman J, Elgoyhen AB, Fuchs PA, Katz E (2011) Short-term synaptic plasticity regulates the level of olivocochlear inhibition to auditory hair cells. J Neurosci 31:14763–14774. CrossRef Medline

Berkefeld H, Fakler B, Schulte U (2010) Ca2+-activated K+ channels: from protein complexes to function. Physiol Rev 90:1437–1459. CrossRef Medline

Beurg M, Evans MG, Hackney CM, Fettiplace R (2006) A large-conductance calcium-selective mechanotransducer channel in mammalian cochlear hair cells. J Neurosci 26:10992–11000. CrossRef Medline

Bond CT, Maylie J, Adelman JP (2005) SK channels in excitability, pacemaking and synaptic integration. Curr Opin Neurobiol 15:305–311. CrossRef Medline

Ehret G (1974) Age-dependent hearing loss in normal hearing mice. Naturwissenschaften 61:506–507. CrossRef Medline

Elgoyhen AB, Johnson DS, Boulter J, Vetter DE, Heinemann S (1994) Alpha 9: an acetylcholine receptor with novel pharmacological properties expressed in rat cochlear hair cells. Cell 79:705–715. CrossRef Medline

Elgoyhen AB, Vetter DE, Katz E, Rothlin CV, Heinemann SF, Boulter J (2001) alpha10: a determinant of nicotinic cholinergic receptor function in mammalian vestibular and cochlear mechanosensory hair cells. Proc Natl Acad Sci U S A 98:3501–3506. CrossRef Medline

Elgoyhen AB, Katz E, Fuchs PA (2009) The nicotinic receptor of cochlear hair cells: a possible pharmacotherapeutic target? Biochem Pharmacol 78:712–719. CrossRef Medline

Engel J, Braig C, Rüttiger L, Kuhn S, Zimmermann U, Blin N, Sausbier M, Kalbacher H, Münkner S, Rohbock K, Ruth P, Winter H, Knipper M (2006) Two classes of outer hair cells along the tonotopic axis of the cochlea. Neuroscience 143:837–849. CrossRef Medline

Evans MG (1996) Acetylcholine activates two currents in guinea-pig outer hair cells. J Physiol 491:563–578. Medline

Fakler B, Adelman JP (2008) Control of K(Ca) channels by calcium nano/microdomains. Neuron 59:873–881. CrossRef Medline

Fettiplace R, Fuchs PA (1999) Mechanisms of hair cell tuning. Annu Rev Physiol 61:809–834. CrossRef Medline

Fiala JC (2005) Reconstruct: a free editor for serial section microscopy. J Microsc 218:52–61. CrossRef Medline

Fuchs PA, Murrow BW (1992) Cholinergic inhibition of short (outer) hair cells of the chick's cochlea. J Neurosci 12:800–809. Medline

Fuchs PA, Sokolowski BH (1990) The acquisition during development of Ca-activated potassium currents by cochlear hair cells of the chick. Proc Biol Sci 241:122–126. CrossRef Medline

Fuchs PA, Lehar M, Hiel H (2014) Ultrastructure of cisternal synapses on outer hair cells of the mouse cochlea. J Comp Neurol 522:717–729. CrossRef Medline

Glowatzki E, Fuchs PA (2000) Cholinergic synaptic inhibition of inner hair cells in the neonatal mammalian cochlea. Science 288:2366–2368. CrossRef Medline

Gómez-Casati ME, Fuchs PA, Elgoyhen AB, Katz E (2005) Biophysical and pharmacological characterization of nicotinic cholinergic receptors in rat cochlear inner hair cells. J Physiol 566:103–118. CrossRef Medline

Hafidi A, Beurg M, Dulon D (2005) Localization and developmental expression of BK channels in mammalian cochlear hair cells. Neuroscience 130: 475–484. CrossRef Medline

Housley GD, Ashmore JF (1991) Direct measurement of the action of acetylcholine on isolated outer hair cells of the guinea pig cochlea. Proc Biol Sci 244:161–167. CrossRef Medline

Im GJ, Moskowitz H, Lehar M, Hiel H, Fuchs P (2014) Synaptic calcium regulation in hair cells of the chicken basilar papilla. J Neurosci 34:16688–16697. CrossRef Medline

Johnson SL, Beurg M, Marcotti W, Fettiplace R (2011) Prestin-driven cochlear amplification is not limited by the outer hair cell membrane time constant. Neuron 70:1143–1154. CrossRef Medline

Katz E, Elgoyhen AB, Gómez-Casati ME, Knipper M, Vetter DE, Fuchs PA, Glowatzki E (2004) Developmental regulation of nicotinic synapses on cochlear inner hair cells. J Neurosci 24:7814–7820. CrossRef Medline

Kelly JB, Masterton B (1977) Auditory sensitivity of the albino rat. J Comp Physiol Psychol 91:930–936. CrossRef Medline

Kong JH, Adelman JP, Fuchs PA (2008) Expression of the SK2 calcium-activated potassium channel is required for cholinergic function in mouse cochlear hair cells. J Physiol 586:5471–5485. CrossRef Medline

Kong WJ, Guo CK, Zhang S, Hao J, Wang YJ, Li ZW (2005) The properties of ACh-induced BK currents in guinea pig type II vestibular hair cells. Hear Res 209:1–9. CrossRef Medline

Kong WJ, Guo CK, Zhang XW, Chen X, Zhang S, Li GQ, Li ZW, Van Cauwenberge P (2007) The coupling of acetylcholine-induced BK channel and calcium channel in guinea pig saccular type II vestibular hair cells. Brain Res 1129:110–115. CrossRef Medline

Kurt S, Sausbier M, Rüttiger L, Brandt N, Moeller CK, Kindler J, Sausbier U, Zimmermann U, van Straaten H, Neuhuber W, Engel J, Knipper M, Ruth P, Schulze H (2012) Critical role for cochlear hair cell BK channels for coding the temporal structure and dynamic range of auditory information for central auditory processing. FASEB J 26:3834–3843. CrossRef Medline

Lee US, Cui J (2010) BK channel activation: structural and functional insights. Trends Neurosci 33:415–423. CrossRef Medline

Lioudyno M, Hiel H, Kong JH, Katz E, Waldman E, Parameshwaran-Iyer S, Glowatzki E, Fuchs PA (2004) A "synaptoplasmic cistern" mediates rapid inhibition of cochlear hair cells. J Neurosci 24:11160–11164. CrossRef Medline

Maison SF, Pyott SJ, Meredith AL, Liberman MC (2013) Olivocochlear suppression of outer hair cells in vivo: evidence for combined action of BK and SK2 channels throughout the cochlea. J Neurophysiol 109:1525–1534. CrossRef Medline

Mammano F, Ashmore JF (1996) Differential expression of outer hair cell potassium currents in the isolated cochlea of the guinea-pig. J Physiol 496:639–646. Medline

Meredith AL, Thorneloe KS, Werner ME, Nelson MT, Aldrich RW (2004) Overactive bladder and incontinence in the absence of the BK large conductance Ca2+-activated K+ channel. J Biol Chem 279:36746–36752. CrossRef Medline

Müller M (1991) Frequency representation in the rat cochlea. Hear Res 51: 247–254. CrossRef Medline

Müller M, von Hünerbein K, Hoidis S, Smolders JW (2005) A physiological place-frequency map of the cochlea in the CBA/J mouse. Hear Res 202: 63–73. CrossRef Medline

Murthy V, Maison SF, Taranda J, Haque N, Bond CT, Elgoyhen AB, Adelman JP, Liberman MC, Vetter DE (2009) SK2 channels are required for function and long-term survival of efferent synapses on mammalian outer hair cells. Mol Cell Neurosci 40:39–49. CrossRef Medline

Oliver D, Klöcker N, Schuck J, Baukrowitz T, Ruppersberg JP, Fakler B (2000) Gating of Ca2+-activated K+ channels controls fast inhibitory synaptic transmission at auditory outer hair cells. Neuron 26:595–601. CrossRef Medline

Pyott SJ, Glowatzki E, Trimmer JS, Aldrich RW (2004) Extrasynaptic localization of inactivating calcium-activated potassium channels in mouse inner hair cells. J Neurosci 24:9469–9474. CrossRef Medline

Pyott SJ, Meredith AL, Fodor AA, Vázquez AE, Yamoah EN, Aldrich RW (2007) Cochlear function in mice lacking the BK channel α, β1, or β4 subunits. J Biol Chem 282:3312–3324. CrossRef Medline

Robitaille R, Charlton MP (1992) Presynaptic calcium signals and transmitter release are modulated by calcium-activated potassium channels. J Neurosci 12:297–305. Medline

Roux I, Wersinger E, McIntosh JM, Fuchs PA, Glowatzki E (2011) Onset of cholinergic efferent synaptic function in sensory hair cells of the rat cochlea. J Neurosci 31:15092–15101. CrossRef Medline

Rüttiger L, Sausbier M, Zimmermann U, Winter H, Braig C, Engel J, Knirsch M, Arntz C, Langer P, Hirt B, Müller M, Köpschall I, Pfister M, Münkner S, Rohbock K, Pfaff I, Rüsch A, Ruth P, Knipper M (2004) Deletion of the Ca^{2+}-activated potassium (BK) alpha-subunit but not the BKbeta1-subunit leads to progressive hearing loss. Proc Natl Acad Sci U S A 101: 12922–12927. CrossRef Medline

Scholl ES, Pirone A, Cox DH, Duncan RK, Jacob MH (2014) Alternative splice isoforms of small conductance calcium-activated SK2 channels differ in molecular interactions and surface levels. Channels (Austin) 8:62–75. CrossRef Medline

Shigemoto T, Ohmori H (1991) Muscarinic receptor hyperpolarizes cochlear hair cells of chick by activating Ca(2+)-activated K+ channels. J Physiol 442:669–690. Medline

Sridhar TS, Brown MC, Sewell WF (1997) Unique postsynaptic signaling at the hair cell efferent synapse permits calcium to evoke changes on two time scales. J Neurosci 17:428–437. Medline

Wang ZW (2008) Regulation of synaptic transmission by presynaptic CaMKII and BK channels. Mol Neurobiol 38:153–166. CrossRef Medline

Wersinger E, Fuchs PA (2011) Modulation of hair cell efferents. Hear Res 279:1–12. CrossRef Medline

Wersinger E, McLean WJ, Fuchs PA, Pyott SJ (2010) BK channels mediate cholinergic inhibition of high frequency cochlear hair cells. PLoS One 5:e13836. CrossRef Medline

Yuhas WA, Fuchs PA (1999) Apamin-sensitive, small-conductance, calcium-activated potassium channels mediate cholinergic inhibition of chick auditory hair cells. J Comp Physiol A 185:455–462. CrossRef Medline

Zorrilla de San Martín J, Pyott S, Ballestero J, Katz E (2010) Ca^{2+} and Ca^{2+}-activated K^+ channels that support and modulate transmitter release at the olivocochlear efferent-inner hair cell synapse. J Neurosci 30:12157–12167. CrossRef Medline